A Novel Approach of Automatic Iridology Chart Drawing onto Eye Images

ICNSE-1451
A Novel Approach of Automatic Iridology Chart Drawing onto Eye Images

A. Anisha[a], J.Y. Huang[b]
[a,b]Graduate Institute of Computer Science and Information Engineering ,
National Taipei University
[a]annisha01@yahoo.com, [b]jiungyao@gmail.com

Abstract

Iridology is an alternative medicine that can tell the health state of an individual organ in a human body by just looking into the eye. Iridologists use the iridology chart as a main reference to perform eye analysis. Traditionally, iridologists have been performing eye analysis in a manual way, which is by using a slit lamp, a magnifying glass, and a plastic iridology chart. As the technology evolves, manual software is developed whereby the chart is drawn onto eye images with the help of a mouse cursor. This work therefore proposes an automatic approach to draw iridology chart automatically onto eye images by using image processing techniques and an iris boundary scanning approach. The goal of this research is to implement an automatic assistant tool for iridologists to perform precise analysis on eye images. Three issues rose when tagging the iridology chart automatically onto an eye image which are the pupil and the iris do not share the same center point, the size of the eye varies for every individual, and the pupil and iris does not have a perfect circle shape.

This paper proposes solution to localize pupil and iris in the eye image first. Parameters of pupil and iris are then determined to compute the transformation matrix to tag the iridology chart correctly onto eye images. Finally, a series of experiments are conducted to validate the proposed approach to successfully localize pupil and iris and hence correctly draw the iridology chart onto eye images automatically.

Keyword: Pupil localization, iris localization, iridology

1. Introduction

Iridology is an alternative medicine which acts as a tool of assessment for disease prevention that can be used to evaluate the health condition of individual organs and also the health level of the body. It is the science and art of reading the texture and features on the iris to predict how healthy or unhealthy every organ in a human body [1]. Iridologists refer, match, and compare their observations of the patterns, spots, color change, and textures on the eye to the iridology chart. Figure 1 is the most recent version of the iridology chart by Dr. David J. Pesek[2].

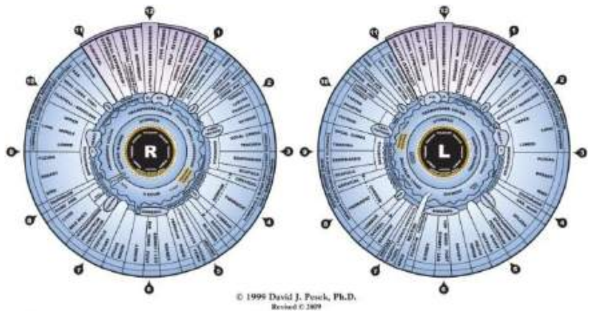

Figure 1: The iridology chart [2]

However, there are several problems that are faced by iridologists and this paper aims to solve the problems. Firstly, iridology analysis is performed on patients manually over the years as it started with the help of a flashlight and a magnifying glass, followed by a plastic iridology chart slided onto eye images. Secondly, the size of the pupil and the iris is different for every human being and hence causes extra work for iridologists to slide the chart according its size. Thirdly, the center point of the pupil and the iris is non-concentric [3]. With the evolvement of technology, assistant software has been developed to draw the iridology chart onto eye images with the help of a mouse cursor to manually localize pupil and iris on eye images [4]. In other words, existing software still require significant effort by the iridologists in order to correctly draw the iridology chart onto eye images. Hence, this paper proposes an approach to automatically and correctly tags the iridology chart onto eye images. This work focuses on three aspects to solve the problem previously mentioned. Firstly iridology chart will be drawn onto eye images automatically. Secondly, image processing techniques are applied to localize the pupil and the iris. Thirdly, affine transformation matrix is applied considering the non-concentricity of the center point of the pupil and the iris.

The organization of this paper is as follows. Section 2 discusses the literature review of this work. Section 3 details the proposed methodology of implementation that consists of three major subsections. Section 4 is about the experimental results that conveys the efficiency of the proposed method in terms of computation time and accuracy and, finally, followed by the conclusion in section 5.

2. Literature Review

Recently, many researches and investigations have been conducted as a contribution to iridology to improve human's health. Ramlee et al. [5] present an approach to detect the presence of cholesterol on eye images. Fuzzy theory also had been employed to analyze disease symptoms to predict its severity [6]. Isak Gath has suggested elliptical shape detection by clustering elliptical shapes of spots on the eye [7]. A semi-automated approach has also been proposed whereby the patterns and colors of the iris are identified and matched to the iridology chart [8]. Furthermore, an iris recognition scheme has been proposed whereby the water flow methodology was adopted [9], [10]. Works have also been done to analyze human iris to detect pulmonary diseases with techniques such as Circular Hough Transform, Fuzzy-C means clustering and gray level analysis [11]. Recently, an automatic healthcare service has been proposed on smartphones to predict the health condition of 4 organs as it emphasizes only to 4 regions in the iridology chart [12]. Similarly, image processing methods have proposed to perform clinical diagnosis on eye images [13]. Although there have been works done on automatic diagnosis focusing on certain diseases based on the iridology chart or certain regions in the iridology chart, there have not been works done focusing on the whole iridology chart automatically.

3. Proposed methodology of implementation

This work is divided into 3 stages which are pupil localization, iris localization, and finally drawing the iridology chart onto the eye image.

3.1 Pupil localization

Pupil localization refers to finding the center point of the pupil, (x_p, y_p) and the radius of the pupil $r_{p.}$ The first step of all is eye image acquisition where eye images are collected by capturing images using an iridologist's camera. 65 images were used in this work [14]. Next, the eye images are converted from the color image to the gray scale image by the luminosity method as shown in equation (1) [15].

$$gray\ scale\ image = 0.299 * R + 0.587 * G + 0.0114 * B \qquad (1)$$

After that, median filter is applied onto the gray scale image in order to smooth the image and reduce the noise caused by light reflection from the camera [16], [17]. Proceeding to the next step, negative function is applied to set apart the pupil region from the eye image for further image processing [18], [19], [20]. Figure 2 illustrated the result after above processes are conducted.

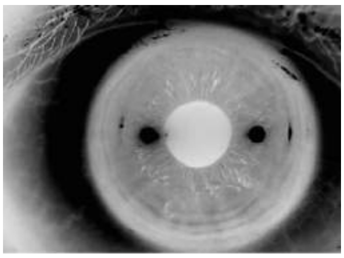

Figure 2: Results after applying negative function

Otsu's thresholding method is applied to find a threshold value where the weighted within-class variance is at its minimum and the between class variance is at its maximum [21], [22], [23]. For accurate segmentation results and for lower computation purposes, Otsu's thresholding was applied only to the bright region of the inverted image that ranges from 155 to 255 because the bright region corresponds to the pupil region. The resulted image is as shown in Figure 3(a). Next, erosion is applied and then followed by dilation to remove the occlusion from the light reflection, eyelashes, and the eyelids [24]. Figure 3(b) depicted the resulted image.

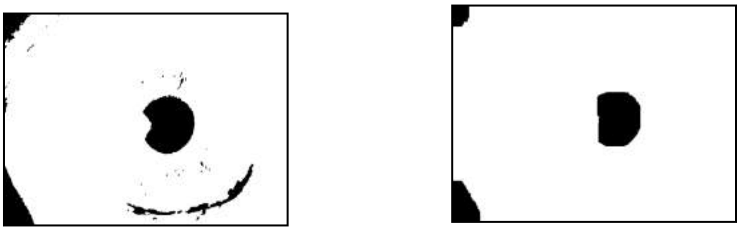

(a) (b)

Figure 3 (a): Binarized eye image after Otsu's thresholding method,
3 (b): After erosion and dilation

Similar to [25], 4-connected component labelling is then applied to group the clusters into distinct labels, calculate the center point of each cluster and hence obtain the cluster that represents the pupil region [26]. The distance of each cluster's midpoint to the image's midpoint is obtained and compared to save the cluster which is the nearest to the midpoint of the image. The center point of that cluster is then saved as the center point of the pupil, (x_p, y_p). After obtaining x_p and y_p, the pixels at the edge along the x-axis and the y-axis x_{min}, y_{min}, x_{max}, and y_{max} are obtained and the radius is calculated by equation (2). At this point, the pupil is eventually localized.

$$r_p = \max\left[\frac{x_{max} - x_{min}}{2}, \frac{y_{max} - y_{min}}{2}\right] \quad (2)$$

3.2 Iris localization

Iris localization refers to finding the center point of the iris, (x_i , y_i) and the radius of the iris r_i. This phase is started with obtaining the gray scale image and then to remove the light reflection spots caused by the iridology camera by setting a threshold value at 160 as proposed in [27]. The resulted image is as shown in Figure 4.

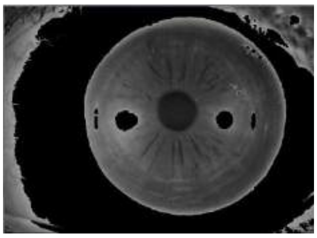

Figure 4: The result after setting a threshold value at 160

4-connected component labelling is then applied again to calculate the area of each cluster to separate the smaller clusters from the largest cluster and, therefore, to set the smaller clusters as 0 in order to cover only the light reflection spots. Next, dilation will be applied to the resulting image to cover up the light refection spots on the eye image as much as possible as shown in Figure 5. After that, an iris boundary scanning approach is proposed to be applied to the region of interest which is within ±30° along the central axis on both left and right sides as similar to the ROI in [18], [28], and [22]. This iris boundary scanning is a straight line scanning that starts from the center point of the pupil at a range of ±30° on both sides of the iris until the first sclera pixel at the range of 180-255 is found. However, some pixels' value of sclera may not lie within this range in the presence of some veins or in the absence of bright illumination around the sclera. So, in order to overcome this, the largest cluster that surrounds the iris, as shown in Figure 4, is saved as 255 in the gray scale image as illustrated in Figure 5. By doing this, any iris boundaries may not be missed. After performing iris boundary scanning, the iris boundary pixels are saved and given labels as (rx_1, ry_1), (rx_2, ry_2), (rx_3, ry_3), (rx_4, ry_4), (rx_5, ry_5), (lx_1, ly_1), (lx_2, ly_2), (lx_3, ly_3), (lx_4, ly_4), and (lx_5, ly_5) as shown in Figure 5.

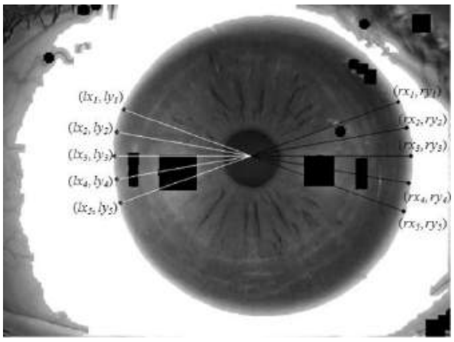

Figure 5: Image that results after reflection spots removal and the iris boundary scanning approach

The average of the points on both sides are then calculated and labeled as (*iris_rx*, *iris_ry*) and (*iris_lx*, *iris_ly*) respectively. After that, the distance between these two points is calculated and, hence, the radius is calculated by equation (3).

$$r_i = \frac{\sqrt{(iris\_lx - iris\_rx)^2 + (iris\_ly - iris\_ry)^2}}{2} \quad (3)$$

Finally, the center point of the iris is calculated by equation (4) and hence the iris is localized.

$$\left(\frac{iris\_rx + iris\_lx}{2}, \frac{iris\_ry + iris\_ly}{2}\right) = (x_i, y_i) \quad (4)$$

3.3 Drawing the iridology chart

Affine transformation is adopted to transform the iridology chart onto an eye image in order to relocate any points from the iridology chart to the eye image [29]. Firstly, 8 pairs of matching control points are obtained to calculate the affine transformation matrix parameters h_{11}, h_{12}, h_{13}, h_{21}, h_{22} and h_{23} where 8 pairs are obtained from the iridology chart and labelled as (A_1, B_1), (A_2, B_2), (A_3, B_3), (A_4, B_4), (A_5, B_5), (A_6, B_6), (A_7, B_7), and (A_8, B_8) and the other 8 are obtained from the pupil and iris localization and hence labelled as (C_1, D_1), (C_2, D_2), (C_3,

D_3), (C_4, D_4), (C_5, D_5), (C_6, D_6), (C_7, D_7), and (C_8, D_8). Next, the origin coordinate is changed to the center point of the pupil in both the iridology chart and the eye image. This is to avoid any scaling problem and to achieve consistent computation for all eye images. Figure 6 illustrates the result of the change in the origin coordinate where (a, b) are the points from the iridology chart and (c, d) are the points from the eye image.

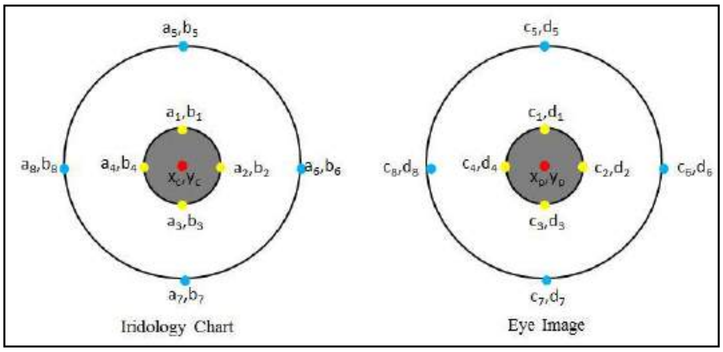

Figure 6: The 8 pairs of matching control points after the change in the origin coordinate.

The 8 pairs of matching control points are then used to obtain the affine transformation matrix variables h_{11}, h_{12}, h_{13}, h_{21}, h_{22} and h_{23} by simultaneous equation solving. Subsequently, any points from the iridology chart can be transformed onto the eye image according to equation (5) where (a, b) represents the points from the chart, and (c, d) represents the points from the eye image. The result of applying affine transformation onto the eye image is as shown in Figure 7.

$$\begin{pmatrix} c \\ d \\ 1 \end{pmatrix} = \begin{pmatrix} h_{11} & h_{12} & h_{13} \\ h_{21} & h_{22} & h_{23} \\ 0 & 0 & 1 \end{pmatrix} * \begin{pmatrix} a \\ b \\ 1 \end{pmatrix} \qquad (5)$$

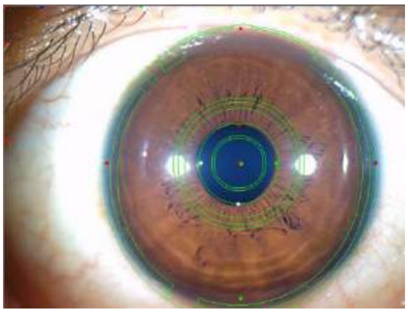

Figure 7: Initial projection of the iridology chart onto the eye image

As can be seen in Figure 7, the iridology chart that is initially projected on the eye image fits well around the iris but it does not fit well around the pupil as some displacements can be seen. To overcome this problem, an equation is derived based on the ratio of the distance of the displaced first six rings from the center point of the pupil. Out of this equation, scale and translation factors are derived as shown in equation (6) to shift only the displaced points to its expected position where (c, d) are the displaced points and (c', d') are the resulting points after shifting the displaced points to its expected location.

$$\begin{pmatrix} c' \\ d' \\ 1 \end{pmatrix} = \begin{pmatrix} S_x & 0 & T_x \\ 0 & S_y & T_y \\ 0 & 0 & 1 \end{pmatrix} \begin{pmatrix} c \\ d \\ 1 \end{pmatrix} \quad (6)$$

Next, the coordinate origin is restored back to the upper-left corner of the image before drawing the chart onto the eye image since the default origin for all images is on the top left. Upon completion, straight lines will be drawn by using simple trigonometry calculation to complete iridology chart.

4. Experimental Results and Performance Analysis

The proposed automatic assistant tool for iridologists is implemented in C and C++ language with Visual Studio 2010 using OpenCV library. The program is tested with 65 images captured using an iridologist's camera [14]. Figure 8 shows the results after drawing the iridology chart onto an eye image automatically.

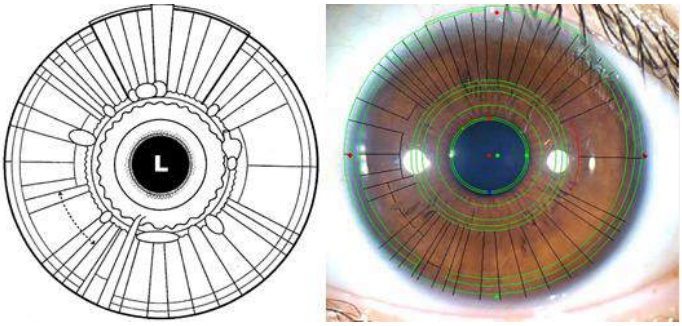

Figure 8: The final iridology chart projected on the eye image for the left eye

Experiments conducted to validate the accuracy of pupil and iris localization and the execution time. For pupil localization, exclusive or operation has been applied on the binarized image and the image after morphological operation to determine the accuracy of pupil localization. The threshold of accuracy is set when the thickness of the ring produced by the exclusive or operation is within 0 to 6 pixels as shown in Figure 9 [30]. For iris localization, the accuracy is measured based on human decision as adopted in [22] with a precision of 3 pixels. If the projected circle exceeds this criterion, then it is considered as false. Table 1 shows the accuracy and the time performance for pupil localization, iris localization and the tagging of the iridology chart onto the eye image. The accuracy for pupil localization is 80% in which errors are caused when the light is in contact with the pupil in the eye image. Uneven distribution of light around the pupil may also cause pupil localization inaccuracy. The accuracy for iris localization is 70.1% in which errors are due to floating-point errors. The accuracy of drawing the chart on the eye image depends on pupil and iris localization. Therefore, the average of the pupil and iris localization is calculated to represent the accuracy of the iridology chart drawing. Accuracy of this work can be improved by three ways. Firstly is by ensuring that the light does not have any contact with the pupil while taking the eye images. Secondly is by avoiding any floating-point errors. Furthermore, the light from the camera should be ensured that it is evenly distributed in between the pupil along the x-axis and the y-axis, or else inaccuracy may occur. Proper illumination is the utmost important as it affects the accuracy of this work and so, precautions needs to be taken while capturing the eye images. The proposed method is therefore proven to have good accuracy with good processing time.

Table 1: Accuracy and processing time of the proposed approach

Stages	Accuracy (%)	Error rate (%)	Processing time (s)
Pupil localization	52/65=80	20	3.281
Iris localization	46/65=70.1	29.9	7.074
Drawing of the chart onto the eye image	(80+70.1)/2 =75.1	24.9	7.373

Figure 9: Results after applying exclusive or operation to Figure 3 (a) and (b)

5. Conclusion

In a nutshell, the iridology chart has been drawn onto eye images automatically with good accuracy and fast time performance. Over the years, there have always been researches and investigations that have been conducted over recent decades as a contribution to iridology to improve human's health because iridology is a non-invasive, simple, and painless method that can be used to access the health condition of every organ in a human body. Future works will be on improvising the accuracy and performance so that it can be implemented on smartphones. Fast localization methods were chosen for this purpose.

References

[1] Elizabeth Micaller, "Emotional Iridology and the Body Mind Connection"

[2] http://www.holisticiridology.com/products/charts/

[3] L. Ma, T. Tan, Y. Wang and D. Zhang, "Efficient Iris Recognition by Characterizing Key Local Variations", IEEE Trans. Image Processing, vol. 13, pp. 739-750, 2004
[4] http://www.szdolma.com/soft/zhizun/CadiCVAdvanceSetup308.rar
[5] R. A. Ramlee and S. Ranjit, "Using Iris Recognition Algorithm, Detecting Cholesterol Presence", Proceedings of International Conference on Information Management and Engineering, IEEE 2009.
[6] Cheng-liang Lai , Chien-lun Chiu, "Health Examination Based On Iris Images", 9th International Conference on Machine Learning and Cybernetics, July 2010.
[7] Isak Gath and Dan Hoory, "Fuzzy clustering of elliptic ring-shaped clusters", Pattern Recognition Letters 16727-741, 1995.
[8] A. Lodin and S. Demea, "Design of an Iris-Based Medical Diagnosis System", Proceeding International Symposium on Signals, Circuits and Systems, pp. 1-4. IEEE 2009.
[9] Othman, Z., A. S. Prabuwono, "Preliminary study on iris recognition system: Tissues of body organs in iridology", IEEE EMBS Conference on Biomedical Engineering & Sciences (IECBES 2010), Kuala Lumpur, 2010, 115–119.
[10] X. Liu, "Image Segmentation Based on Water Flow Analogy", PHD Thesis, University of Southampton, 2009.
[11] K. Sivasankar, M. Sujaritha, P. Pasupathi, S. Muthukumar, "FCM based Iris Image Analysis for Tissue Imbalance Stage Identification", International Conference on Emerging Trends in Science, Engineering and Technology 2012.
[12] D. H. Hareva, S. Lukas, N. O. Suharta, "The Smart Device for Healthcare Service: Iris Diagnosis Application", 11th International Conference on ICT and Knowledge Engineering 2013.
[13] Jogi, Sandeep Panwar, and Bharat Bhushan Sharma. "Methodology of iris image analysis for clinical diagnosis", Medical Imaging, m-Health and Emerging Communication Systems (MedCom), 2014 International Conference on. IEEE, 2014.
[14] https://www.dropbox.com/sh/r1wqd3zb9uoc5o1/AAA7IGU9o7OAQoaRLYBdguIma?dl=0
[15] http://zerocool.is-a-geek.net/java-color-image-to-grayscale-conversion-algorithm/
[16] Parker, Jim R., "Algorithms for image processing and computer vision", John Wiley & Sons, 2010.
[17] Phillips, Dwayne. "Image processing in C", Vol. 724. R & D Publications, 1994.
[18] R. P. Ramkumar, S Arumugam, "A Novel Iris Recognition Algorithm", Computing Communication & Networking Technologies (ICCCNT), (2012) 1-6.
[19] Almisreb, Ali Abd, Nooritawati Md Tahir, and Mustaffa Samad, "Pupil Localization Using Negative Function and the Four Neighbors", Computational Intelligence, Modelling and Simulation (CIMSiM), 2010 Second International Conference on. IEEE,

2010.

[20] Ali Abd Almisreb, Nooritawati Md Tahir, Adzrool Idzwan Ismail, and Ramli Abdullah, “Enhancement Pupil Isolation Method in Iris Recognition”, IEEE International Conference on System Engineering and Technology (lCSEr), pp.I-4, 2011.

[21] Otsu, N. “A threshold selection method from gray-level histograms”, IEEE Trans. Systems, Man, and Cybernetics 9(1), 62–66 (1979).

[22] Tariq. M. Khan, M. Aurangzeb Khan, S. A. Malik, S. A. Khan, T. Bashir, and A. H. Dar, “Automatic localization of pupil using eccentricity and iris using gradient based method”, Optics and Lasers in Engineering, vol. 49, pp. 177-187, 2011.

[23] http://www.labbookpages.co.uk/software/imgProc/otsuThreshold.html

[24] Gonzalez, Rafael C., “Digital image processing”, Pearson Education India, 2009.

[25] N.S.N.B. Puhan and X. Jiang, “Robust Eyeball Segmentation in Noisy Iris Images Using Fourier Spectral Density”, Proc. Sixth IEEE Int',l Conf. Information, Comm., and Signal Processing, pp. 1-5, 2007.

[26] Acharya, Tinku, and Ajoy K. Ray. “Image processing: principles and applications”, John Wiley & Sons, 2005.

[27] M. A. M. Abdullah, S. S. Dlay, and W. L. Woo, “Fast and Accurate Pupil Isolation Based on Morphpology and Active Contour”, 4th International Conference on Signal, Image Processing and Applications, Nottingham, UK, 2014, pp. 418-420.

[28] Kittipol Horapong, Jirayut Sreecholpech, Somying Thainimit, Vutipong Areekul, “An Iris Verification Using Edge Detection”, ICICS 2008, pp.1434-1438, 2008.

[29] Shapiro, Linda, and George C. Stockman, “Computer Vision. 2001”, Prentice Hall, 2001.

[30] http://www.cplusplus.com/doc/boolean/